Noninvasive Cuffless Estimation of Blood Pressure from Pulse Arrival Time and Heart Rate with Adaptive Calibration

Federico S. Cattivelli
Department of Electrical Engineering
University of California, Los Angeles
Los Angeles, USA
e-mail: fcattiv@ee.ucla.edu

Harinath Garudadri
Qualcomm
San Diego, USA
e-mail: hgarudad@qualcomm.com

***Abstract*—We study the problem of noninvasively estimating Blood Pressure (BP) without using a cuff, which is attractive for continuous monitoring of BP over Body Area Networks. It has been shown that the Pulse Arrival Time (PAT) measured as the delay between the ECG peak and a point in the finger PPG waveform can be used to estimate systolic and diastolic BP. Our aim is to evaluate the performance of such a method using the available MIMIC database, while at the same time improve the performance of existing techniques. We propose an algorithm to estimate BP from a combination of PAT and heart rate, showing improvement over PAT alone. We also show how the method achieves recalibration using an RLS adaptive algorithm. Finally, we address the use case of ECG and PPG sensors wirelessly communicating to an aggregator and study the effect of skew and jitter on BP estimation.**

***Keywords*—Cuffless, Pulse Transit Time, Pulse Arrival Time, MIMIC**

I. Introduction

Measurement of arterial blood pressure (BP) involves obtaining the systolic blood pressure (SBP) and diastolic blood pressure (DBP), defined as the highest and lowest pressures during a cardiac cycle. The golden standard to measure BP is the ausculatory method, where a specialist inflates a cuff around the arm, and uses a stethoscope to determine SBP and DBP. Oscillometric techniques are based on the same principle, but are intended for home use. These two methods require the use of a cuff, which is bulky, costly, and does not allow continuous monitoring.

In this work we consider cuff-less, non-invasive BP estimation. It has been shown that Pulse Arrival Time (PAT), measured as the delay between QRS peaks in ECG and corresponding points in the photoplethysmogram (PPG) waveform, can be used to estimate SBP and DBP [1]-[3]. This technique is attractive in the context of Body Area Networks (BANs), where a set of sensors are placed on the human body in order to monitor vital signs (see Fig. 1). Both ECG and PPG signals can be obtained using low-cost, low-power sensors.

Our contributions are as follows. First, we propose an adaptive algorithm to estimate SBP and DBP without using a cuff. Second, we show that using instantaneous heart-rate in addition to PAT can improve the performance. Third, we evaluate our estimation algorithms on the publicly available MIMIC database [4]. Finally, we study the effect of signal skew and jitter on estimation performance. This is specially relevant in the context of BANs, where the signals arriving from different sensors may have unknown time skews, since individual sensors have their own radios. Synchronizing wireless sensors to an arbitrarily fine resolution of clock will have an impact on both cost and life of the sensors.

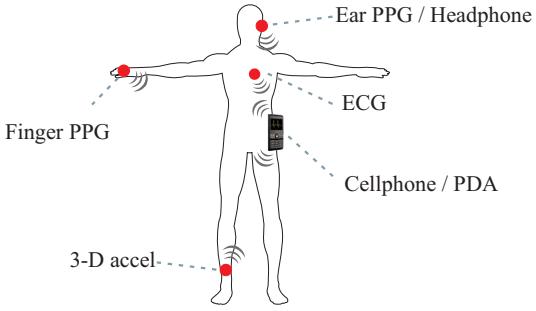

Fig. 1. Example Body Area Network.

II. Background

Pressure waves produced at the heart propagate through the arteries at a certain velocity known as the pulse-wave velocity, which depends on the elastic properties of arteries and blood. The Moens-Korteweg equation gives the pulse-wave velocity as a function of vessel and fluid characteristics:

$$c = \frac{L}{PTT} = \sqrt{\frac{E \cdot h}{\rho 2R}} \qquad (1)$$

where c is the wave velocity, L is the length of the vessel, PTT (Pulse Transit Time) is the time it takes for a pressure pulse to transit through that length, ρ is the fluid density, R is the inner radius of the vessel, E is the modulus of wall elasticity (Young's modulus), and h is the vessel thickness. For an elastic vessel, there exists an empirical exponential relation between E and the fluid pressure P [5], [1], namely $E = E_0 e^{\alpha(P-P_0)}$ where E_0 and P_0 are nominal values of Young's modulus and pressure, respectively, and α is some constant. From (1) we obtain that there is a logarithmic

978-0-7695-3644-6/09 $25.00 © 2009 IEEE
DOI 10.1109/BSN.2009.35

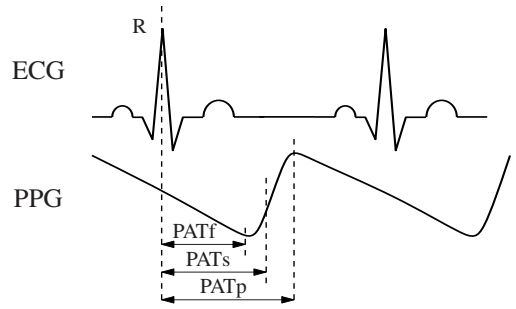

Fig. 2. PAT measured between R peak of ECG and a particular point of PPG.

relation between blood pressure and PTT. Another model commonly used can be derived for small changes of PTT around a nominal value PTT_0. Linearizing the logarithmic model we obtain:

$$\text{BP} = a\text{PTT} + b \tag{2}$$

Different models have been used in the literature to estimate BP. In our work, we focus on linear models of the form (2), not because they provide a better fit, but because they have been observed to be more robust to noisy measurements.

PTT is typically measured indirectly through a related quantity known as Pulse Arrival Time (PAT). PAT is calculated as the delay between the R peak of ECG and a particular point in the photoplethysmogram (PPG) signal, such as the foot (PATf), peak (PATp) or maximum slope point (PATs) (see Fig. 2). PAT is related to PTT as follows [1]

$$\text{PAT} = \text{PEP} + \text{PTT}$$

where PEP is the Pre-Ejection Period. PEP represents the isovolumetric contraction time of the heart, which is the time it takes for the myocardium to raise enough pressure to open the aortic valve and start pushing blood out of the ventricle. Only PTT is related to BP through relation (1). It has been noted before [3], [6] that the effect of PEP on PAT is significant, and that using PAT to estimate BP would be unreliable. Nonetheless, good correlations between BP and PAT have been consistently observed in the literature.

The Association for the Advancement of Medical Instrumentation (AAMI) requirements for BP estimation indicate that the mean of the estimation error has to be lower than 5 mmHg in absolute value, and that the standard deviation of the error has to be below 8 mmHg, both for SBP and DBP.

III. Methodology

We have empirically observed that for some records in the MIMIC database, BP is highly correlated with instantaneous heart-rate (HR). As heart rate increases, so does the cardiac output flow, and therefore if the arteries are considered to be purely resistive, BP would increase linearly with HR. Thus, in conjunction with model (2) we propose the following observation model:

$$\begin{aligned} \text{SBP} &= a_1 \cdot \text{PAT} + b_1 \cdot \text{HR} + c_1 \\ \text{DBP} &= a_2 \cdot \text{PAT} + b_2 \cdot \text{HR} + c_2 \end{aligned} \tag{3}$$

where $\{a_1, a_2, b_1, b_2, c_1, c_2\}$ are unknown parameters. Calibration of these parameters is done in two steps. First, an initial, per-user calibration is performed, using a number of measurements of SBP and DBP. Second, the parameters are adaptively re-calibrated by taking one new measurement every T_{cal} seconds.

A. Initial calibration

Initial calibration is performed the first time the subject uses the system for BP estimation. Our results indicate that about 10 to 40 measurements are needed for initial calibration in order to obtain good performance. Calibration can be achieved through a least-squares procedure as follows. We group the unknown parameters into a matrix θ such that

$$\theta = \begin{bmatrix} a_1 & a_2 \\ b_1 & b_2 \\ c_1 & c_2 \end{bmatrix} \tag{4}$$

Given N observations of $\text{SBP}(i)$, $\text{DBP}(i)$, $\text{PAT}(i)$ and $\text{HR}(i)$, from time instants $i = i_1, \ldots, i_N$, we collect these observations into matrices

$$Y_{1:N} = \begin{bmatrix} \text{SBP}(i_1) & \text{DBP}(i_1) \\ \vdots & \vdots \\ \text{SBP}(i_N) & \text{DBP}(i_N) \end{bmatrix}$$

$$X_{1:N} = \begin{bmatrix} \text{PAT}(i_1) & \text{HR}(i_1) & 1 \\ \vdots & \vdots & \vdots \\ \text{PAT}(i_N) & \text{HR}(i_N) & 1 \end{bmatrix}$$

The value of θ that minimizes $||Y_{1:N} - X_{1:N}\theta||^2$ is [7]

$$\theta_N = [X_{1:N}^T X_{1:N}]^{-1} X_{1:N}^* Y_{1:N} \tag{5}$$

Given a new set of measurements X, we can obtain an estimate of Y, denoted by $\hat{Y}$, as $\hat{Y} = X\theta_N$. Let P_N denote the inverse of the correlation matrix of the initial estimate, i.e.,

$$P_N = [X_{1:N}^* X_{1:N}]^{-1} \tag{6}$$

B. Adaptive re-calibration

It has been observed that the estimation performance of cuffless BP algorithms remains accurate within a certain period after calibration [8], and that re-calibration may be required after this period. Re-calibration requires the user to take one measurement of SBP and DBP, using for example a cuff-based oscillometric device available for home use. Our results indicate that the calibration period should be at most 1 hour 20 min to provide good results (see Sec. IV-A).

Let T_{cal} denote the time interval between consecutive calibration instances, and i_{N+1} denote the first re-calibration

instant after the initial calibration. Note that i_N and i_{N+1} are arbitrary time instants and need not be contiguous. Then, given a new set of observations $SBP(i_{N+1})$, $DBP(i_{N+1})$, $PAT(i_{N+1})$ and $HR(i_{N+1})$, we can incorporate these new measurements into the least-squares problem (5) by using the RLS algorithm recursions. That is, the solution that minimizes the cost $||Y_{1:N+1} - X_{1:N+1}\theta||^2$ can be found from [7]:

$$\begin{aligned} \theta_{N+1} &= \theta_N + \frac{\lambda^{-1} P_N u_{N+1}^* (d_{N+1} - u_{N+1}\theta_N)}{1+\lambda^{-1} u_{N+1} P_N u_{N+1}^*} \\ P_{N+1} &= P_N - \frac{\lambda^{-2} P_N u_{N+1}^* u_{N+1} P_N}{1+\lambda^{-1} u_{N+1} P_N u_{N+1}^*} \end{aligned} \quad (7)$$

where

$$\begin{aligned} d_{N+1} &= [SBP(i_{N+1}) \quad DBP(i_{N+1})] \\ u_{N+1} &= [PAT(i_{N+1}) \;\; HR(i_{N+1}) \;\; 1] \end{aligned}$$

and λ is a forgetting factor, typically chosen $0 \ll \lambda \leq 1$. In our experiments we use $\lambda = 0.95$.

C. Enhancing robustness

We have observed that in some instances the measurements of SBP, DBP, PAT and HR can be very noisy, and thus may produce estimates of θ which are in some cases not physically possible. Thus, we have adopted a mechanism to enhance robustness, whereby the parameters a_1, a_2, b_1 and b_2 are kept within certain limits. Whenever a parameter obtained through (5) or (7) is outside of the allowed range, it is rounded to the closest point in that range. We denote the minimum and maximum parameters as θ_{min} and θ_{max}, respectively. Depending on the correlations between the observations, we allow these ranges to change as we show next. Particularly, we have adopted the following allowed ranges for the parameters

$$\theta_{0,min} = \begin{bmatrix} -400 & -300 \\ 0 & 0 \\ -\infty & -\infty \end{bmatrix}, \theta_{0,max} = \begin{bmatrix} 0 & 0 \\ 2 & 2 \\ \infty & \infty \end{bmatrix}$$
$$\theta_{min} = \min(\theta_{0,min}, (1-\rho) \odot \theta_{0,min} + \rho \odot \theta_N)$$
$$\theta_{max} = \max(\theta_{0,max}, (1-\rho) \odot \theta_{0,max} + \rho \odot \theta_N)$$

where $\odot$ represents element-wise multiplication and θ_N is the parameter obtained after the initial calibration. ρ is a matrix such that

$$\rho = \begin{bmatrix} \rho_{PAT} & 0 \\ \rho_{HR} & 0 \\ 0 & 0 \end{bmatrix} \quad (8)$$

where ρ_{PAT} is the absolute correlation coefficient between SBP and PAT, and ρ_{HR} is the absolute correlation coefficient between SBP and HR. These coefficients are obtained during the initial calibration. Thus, whenever PAT and SBP are strongly correlated and $\rho_{PAT} \approx 1$, if the value of a_1 obtained through calibration is below the required limit, this limit will be reduced to accommodate larger variations. This approach has the advantage of avoiding restricting a_1 for those patients where a_1 is strongly correlated with SBP, and therefore should be kept unaltered. We denote by η_{N+1} the fixed version of θ_{N+1}, i.e.,

$$\eta_{N+1} = \min(\theta_{max}, \max(\theta_{min}, \theta_{N+1})) \quad (9)$$

D. Fixing the bias

After we adapt the parameters through (7) and fix them to be within their allowed ranges through (9), we need to fix c_1 and c_2, which correspond to the bias term. We will denote the resulting estimate as γ_{N+1}. The first two rows of η_{N+1} are kept unmodified, i.e.,

$$e_1^T \gamma_{N+1} = e_1^T \eta_{N+1} \qquad e_2^T \gamma_{N+1} = e_2^T \eta_{N+1} \quad (10)$$

where e_k is a vector with a unity entry in position k, and zeros elsewhere. For the last row of γ_{N+1}, we have

$$e_3^T \gamma_{N+1} = \alpha e_3^T \eta_{N+1} + (1-\alpha)(d_{N+1} - \tilde{u}_{N+1}\tilde{\eta}_{N+1}) \quad (11)$$

where

$$\begin{aligned} \tilde{u}_{N+1} &= [PAT(i_{N+1}) \;\; HR(i_{N+1})] \\ \tilde{\eta}_{N+1} &= [I_2 \;\; 0]\, \eta_{N+1} \end{aligned}$$

and $\alpha = 0.3$ has been observed to provide good results.

After we obtain γ_{N+1}, we can estimate BP at an arbitrary time instant k as $\hat{d}_k = u_k \gamma_{N+1}$. The complete proposed algorithm is given by Eqns. (5)-(11), and we will refer to it as "Algorithm 1".

IV. Results

We applied our proposed Alg. 1 on the MIMIC database, using signals upsampled to 1kHz. For the initial calibration stage, we used 40 measurements of SBP and DBP, spaced 5 minutes apart. Unless otherwise noted, we re-calibrated every $T_{cal} = 1$ hour.

Of the 72 records available in the MIMIC database, only 56 have complete recordings of PPG, ECG and ABP. Of these, 22 were removed because of abnormal ECG waveforms or extensive movement artifacts. The rationale for excluding these records is that we want to test the feasibility of estimating BP from PAT, assuming that the PPG signals are clean enough for us to detect their peaks and valleys. Thus, we worked with 34 records coming from 25 different patients.

Table IV shows mean and standard deviation of the SBP and DBP estimation errors, averaged over all 34 records, for T_{cal}=1 hour, and for 6 different algorithms. The first algorithm, denoted by "No est." is a trivial estimator, where the estimated values of SBP and DBP are equal to the measurements obtained in the latest calibration. The remaining algorithms are based on our proposed Alg. 1, but they use different types of measurements. The algorithm denoted by "PATp only" uses only PAT peaks, and ignores other measurements. We also remove the coefficient range correction. The algorithms denoted by "PATs only", "PATf only"

TABLE I
ERROR MEAN, ERROR STANDARD DEVIATION (S.D.) AND MEAN-SQUARE ERROR (MSE) FOR DIFFERENT ALGORITHMS, AVERAGED OVER ALL RECORDS. † MSE HAS UNITS OF MMHG^2.

	SBP (mmHg)			DBP (mmHg)		
Algorithm	**mean**	**s.d.**	**mse** †	**mean**	**s.d.**	**mse** †
No est.	0.13	9.55	104.12	0.08	5.81	47.77
PATp only	-0.18	8.37	81.93	0.01	5.18	38.56
PATs only	-0.31	8.08	76.97	-0.01	5.11	37.30
PATf only	-0.28	8.94	93.06	-0.05	5.30	39.11
HR only	-0.22	8.56	87.05	-0.03	5.05	36.15
Alg. 1	-0.41	7.77	70.05	-0.07	4.96	35.08

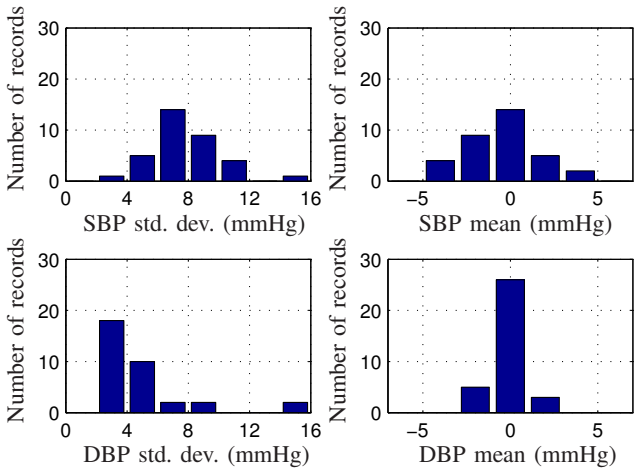

Fig. 3. Histograms of estimation error statistics for SBP and DBP, using Alg. 1.

and"HR only" are the same as the one previously described, except that they use PAT maximum slope point, PAT foot and HR, respectively, instead of PATp. The algorithm denoted by "Alg.1" is the fully implemented Alg. 1, which uses PATs and HR.

We observe that among all the PAT methods, PATs is the best in terms of minimizing the standard deviations. Moreover, using HR only has similar performance to using PATp only. Among all the methods, Alg. 1 obtains the best performance with respect to the standard deviations, since it combines both PATs and HR.

Fig. 3 shows the distributions of the error mean and standard-deviation for all records, using Alg. 1. All records have error means between -5 and 5 mmHg, both for SBP and DBP. Regarding the standard deviations of DBP, most records are below 8mmHg, and four records do not meet this requirement. For SBP, 14 records did not meet the requirement.

Fig. 4 shows the measured and estimated blood pressure waveforms for a portion of record 212. It can be seen that the signals are in close agreement in this case, and the estimated waveform follows closely the trends of the measured pressure.

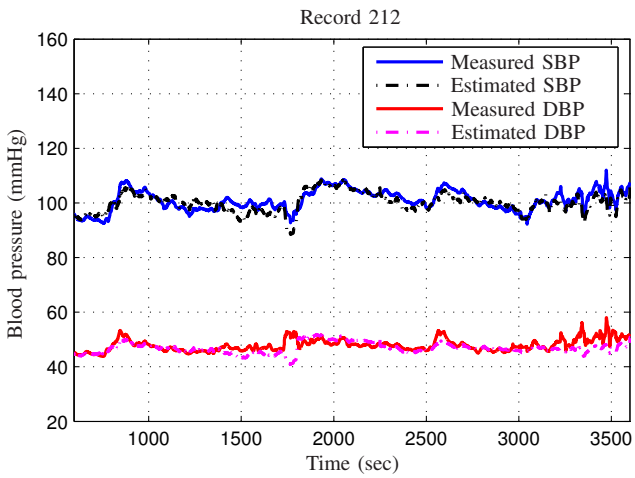

Fig. 4. Actual and estimated SBP and DBP using Alg.1, for part of record 212.

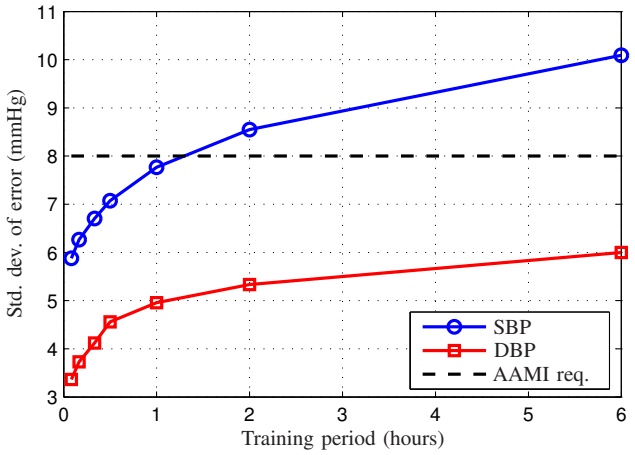

Fig. 5. Standard deviation of SBP and DBP error vs. calibration period, T_{cal}.

A. *Effect of calibration time*

We now study the effect of the calibration period, T_{cal}, on the estimation performance. T_{cal} denotes the time interval between consecutive re-calibration instances. More frequent calibrations will reduce the error while less frequent calibrations will make the system more amenable for everyday use. Fig. 5 shows the standard deviation of the estimation error, both for SBP and DBP, as a function of T_{cal}. The plot also indicates that in order to attain less than 8 mmHg in the error standard deviation, on average, T_{cal} should be about 1 hour and 20 min.

B. *Effect of skew*

We now study the effect of skew on estimation performance. In the setup of Fig. 1, sensors take their measurements and communicate them to a concentrator (e.g., PDA or

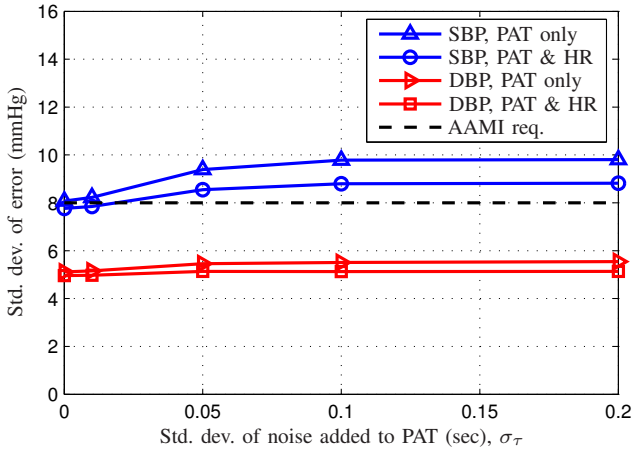

Fig. 6. Standard deviation of SBP and DBP error vs. added random PAT skew, using $T_{cal} = 1$ hour.

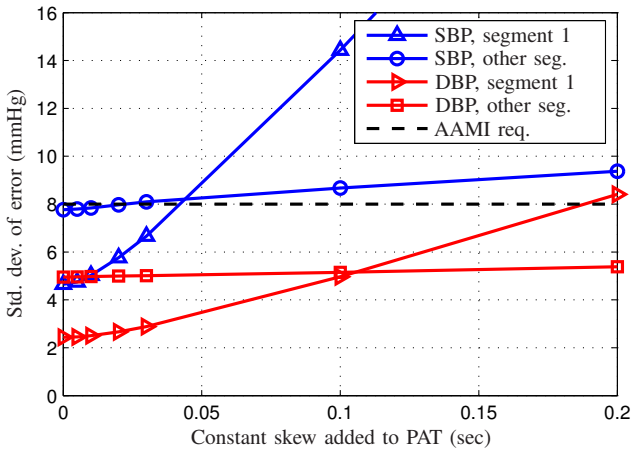

Fig. 7. Std. dev. of SBP and DBP error vs. added PAT skew, using $T_{cal} = 1$ hour.

cellphone) for processing. Since the sensors operate independent of each other, there will exist some temporal mismatch between the measurements received at the concentrator. In a cuffless BP application, where the estimation is based on the delay between two signals coming from different sensors, the time mismatch at the concentrator due to the communication channels becomes important. In our context, skew refers to any time error produced when calculating the Pulse Arrival Time. We study what is the penalty in BP estimation as we artificially add skew to the PAT.

1) Random skew: Random skew represents random variations in the synchronization of the two signals, caused by clock jitter, processing delay, etc. A typical solution to mitigate jitter is to use a de-jitter buffer at the receiver at the cost of some additional latency. The buffer is drained at a constant rate, for a given application. The added random skew is modeled as white, zero-mean Gaussian, with standard deviation σ_τ. Fig. 6 shows the standard deviation of the estimation error, for SBP and DBP, as a function of the standard deviation of the added skew. We show results for two algorithms: Alg. 1, which uses PAT and HR, and a version that uses only PAT.

We observe that the skew degrades the performance of the algorithms, up to a point where the degradation saturates. This represents the point where PAT is too noisy and the algorithm stops using this measurement for estimation. Note that since HR is measured from one signal only (either ECG or PPG), there is no additional skew introduced in this signal due to the communication system. Thus, the method that uses both PAT and HR has advantages over the method that uses PAT only, as shown in Fig. 6. This makes the former method attractive for BAN implementations, since it does not degrade significantly with PAT. On average, this method remains within the AAMI requirements, for skews up to about 20ms.

2) Constant skew: Constant skew occurs at the receiver when PPG and ECG de-jitter buffers are not adequately coordinated. This is analogous to audio/visual synchronization when audio and video data are received over channels with different properties. In order to study the effect of constant skew, we perform the initial calibration of the system using measurements without skew. Subsequently, we introduce a constant skew to the PAT, and run the estimation algorithm. We are interested in two quantities. First, we would like to find out how the skew affects the estimation performance before any re-calibration is performed. Second, we want to know how re-calibration will deal with the skew, and if it will be able to mitigate it. In order to analyze these effects, we proceed as follows. After we calibrate the system for each record, we run the estimation algorithm over one segment of duration $T_{cal} = 1$ hour, without re-calibration. Then we record the standard deviation and mean of the error on this first segment, which we refer to as "segment 1". Subsequently, we allow our re-calibration algorithm to work on the signal, and record the standard deviation and mean of the error for all subsequent segments in the record (excluding segment 1).

Fig. 7 shows the effect of skew on the standard deviation of the error, for SBP and DBP, and also for segment 1 and the remaining segments, as a function of the amplitude of the added skew. It is interesting to note that both SBP and DBP estimates degrade considerably for segment 1 as we increase the skew. Nonetheless, the standard deviation for the remaining segments does not change much as we increase the amplitude of the skew. This indicates that the re-calibration algorithm is doing its job correctly, and is able to correct the skew after a few instances (our experiments show that one re-calibration is usually good enough). Constant skews of about 20ms would be tolerable in order to be within the AAMI requirements for standard deviation, on average.

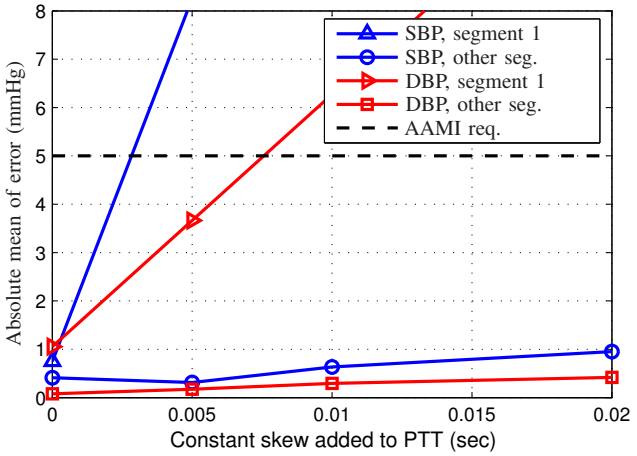

Fig. 8. Absolute mean of SBP and DBP error vs. added PAT skew, using $T_{cal} = 1$ hour.

Fig. 8 shows the effect of skew on the absolute mean of the error, for SBP and DBP, and also for segment 1 and the remaining segments, as a function of the amplitude of the added skew. Again, SBP and DBP estimates degrade considerably for segment 1 as we increase the skew, and the degradation is more significant than that of the standard deviation. Skews of about 2-3ms would be tolerable to be within the AAMI requirements, on average. However, as was the case before, the absolute mean for the remaining segments remains within the required 5mmHg, indicating that the skew is being corrected after re-calibration.

V. Conclusions

We proposed an algorithm to estimate SBP and DBP using PAT and instantaneous heart rate. After an initial training, the model parameters are re-calibrated in constant intervals using an RLS approach combined with smooth bias fixing. The algorithm was applied on the MIMIC database, where we found that our algorithm provides average SBP and DBP standard deviations of 7.77mmHg and 4.96mmHg, respectively, with recalibration every 1 hour.

We also showed that using heart-rate as well as PAT provides more robustness to random skews (since heart rate is insensitive to skew), and in this case standard deviations of about 20ms could be tolerated. Constant skews produce significant degradation if left unaccounted, and should not exceed 2-3ms . However, this effect is mitigated after re-calibration.

References

[1] W. Chen, T. Kobayashi, S. Ichikawa, Y. Takeuchi, and T. Togawa, "Continuous estimation of systolic blood pressure using the pulse arrival time and intermittent calibration," *Med. Biol. Eng. Comput.*, vol. 38, 2000.

[2] C. Poon and Y. Zhang, "Cuff-less and noninvasive measurements of arterial blood pressure by pulse transit time," in *Proc. IEEE EMBS Conf.*, Shanghai, China, September 2005, pp. 5877–5880.

[3] J. Muehlsteff, X. Aubert, and M. Schuett, "Cuffless estimation of systolic blood pressure for short effort bicycle tests: The prominent role of the pre-ejection period," in *Proc. IEEE EMBS Conf.*, NY, August 2006.

[4] G. B. Moody and R. G. Mark, "A database to support development and evaluation of intelligent intensive care monitoring," in *Proc. Computers in Cardiology*, Indianapolis, IN, September 1996, pp. 657–660.

[5] D. J. Hughes, L. A. Geddes, C. F. Babbs, and J. D. Bourland, "Measurements of young's modulus of the canine aorta in-vivo with 10 mhz ultrasound," in *Proc. Ultrasonics Symposium*, September 1978, pp. 326– 326.

[6] R. A. Payne, C. N. Symeonides, D. J. Webb, and S. R. J. Maxwell, "Pulse transit time measured from the ecg: an unreliable marker of beat-to-beat blood pressure," *J. Appl. Physiol.*, vol. 100, pp. 163–141, 2006.

[7] A. H. Sayed, *Fundamentals of Adaptive Filtering*. NJ: Wiley, 2003.

[8] P. Shaltis, A. Reisner, and H. Asada, "Calibration of the photoplethysmogram to arterial blood pressure: Capabilities and limitations for continuous pressure monitoring," in *Proc. IEEE EMBS Conf.*, Shanghai, China, September 2005, pp. 3970–3973.